



The H3 histone chaperone NASP SIM3 escorts CenH3 in Arabidopsis

Samuel Le Goff, Burcu Nur Keçeli, Hana Jeřábková, Stefan Heckmann, Twan Rutten, Sylviane Cotterell, Veit Schubert, Elisabeth Roitinger, Karl Mechtler, F. Christopher H. Franklin, et al.

► To cite this version:

Samuel Le Goff, Burcu Nur Keçeli, Hana Jeřábková, Stefan Heckmann, Twan Rutten, et al.. The H3 histone chaperone NASP SIM3 escorts CenH3 in Arabidopsis. *Plant Journal*, 2019, 10.1111/tpj.14518 . hal-02323987

HAL Id: hal-02323987

<https://hal.science/hal-02323987>

Submitted on 21 Oct 2019









HAL is a multi-disciplinary open access archive for the deposit and dissemination of scientific research documents, whether they are published or not. The documents may come from teaching and research institutions in France or abroad, or from public or private research centers.

L'archive ouverte pluridisciplinaire **HAL**, est destinée au dépôt et à la diffusion de documents scientifiques de niveau recherche, publiés ou non, émanant des établissements d'enseignement et de recherche français ou étrangers, des laboratoires publics ou privés.



Distributed under a Creative Commons Attribution 4.0 International License

The H3 histone chaperone NASP^{SIM3} escorts CenH3 in Arabidopsis

Samuel Le Goff^{1,†} , Burcu Nur Keçeli^{2,†} , Hana Jeřábková³ , Stefan Heckmann⁴ , Twan Rutten⁴ , Sylviane Cotterell¹ , Veit Schubert⁴ , Elisabeth Roitinger^{5,6,7} , Karl Mechtler^{5,6,7} , F. Christopher H. Franklin⁸ , Christophe Tatout¹ , Andreas Houben⁴ , Danny Geelen² , Aline V. Probst^{1,*}  and Inna Lermontova^{4,9,*} 

¹GRoD, Université Clermont Auvergne, CNRS, INSERM, BP 38, 63001, Clermont-Ferrand, France,

²Department of Plants and Crops, Unit HortiCell, Faculty of Bioscience Engineering, Ghent University, Coupure links, 653, 9000, Ghent, Belgium,

³The Czech Academy of Sciences, Institute of Experimental Botany (IEB), Centre of the Region Haná for Biotechnological and Agricultural Research, Šlechtitelů 31, 78 371, Olomouc, Czech Republic,

⁴Leibniz Institute of Plant Genetics and Crop Plant Research (IPK) Gatersleben, Corrensstrasse 3, D-06466, Seeland, Germany,

⁵Institute of Molecular Pathology (IMP), Vienna BioCenter (VBC), Vienna 1030, Austria,

⁶Institute of Molecular Biotechnology (IMBA), Austrian Academy of Sciences, Vienna BioCenter (VBC), Vienna 1030, Austria,

⁷Gregor Mendel Institute (GMI), Austrian Academy of Sciences, Vienna BioCenter (VBC), Vienna 1030, Austria,

⁸School of Biosciences, University of Birmingham, Edgbaston, Birmingham B15 2TT, UK, and

⁹Mendel Centre for Plant Genomics and Proteomics, CEITEC, Masaryk University, Brno CZ-62500, Czech Republic

Received 10 April 2019; revised 16 August 2019; accepted 21 August 2019.

*For correspondence (e-mails aline.probst@uca.fr and lermonto@ipk-gatersleben.de).

[†]These authors contributed equally to this work.

SUMMARY

Centromeres define the chromosomal position where kinetochores form to link the chromosome to microtubules during mitosis and meiosis. Centromere identity is determined by incorporation of a specific histone H3 variant termed CenH3. As for other histones, escort and deposition of CenH3 must be ensured by histone chaperones, which handle the non-nucleosomal CenH3 pool and replenish CenH3 chromatin in dividing cells. Here, we show that the Arabidopsis orthologue of the mammalian NUCLEAR AUTOANTIGENIC SPERM PROTEIN (NASP) and *Schizosaccharomyces pombe* histone chaperone Sim3 is a soluble nuclear protein that binds the histone variant CenH3 and affects its abundance at the centromeres. NASP^{SIM3} is co-expressed with Arabidopsis CenH3 in dividing cells and binds directly to both the N-terminal tail and the histone fold domain of non-nucleosomal CenH3. Reduced NASP^{SIM3} expression negatively affects CenH3 deposition, identifying NASP^{SIM3} as a CenH3 histone chaperone.

Keywords: *Arabidopsis thaliana*, centromere, kinetochore, CenH3, histone chaperone, NASP^{SIM3}.

INTRODUCTION

Eukaryotic DNA is organized into chromatin using histones as components of its building blocks, the nucleosomes. The incorporation of different histone variants into the nucleosome determines nucleosome stability, DNA accessibility and higher order chromatin organization. The histone variant CenH3 is unique in that its incorporation is limited to the centromeres (Talbert *et al.*, 2002; Lermontova *et al.*, 2015; Rosin and Mellone, 2017). CenH3 deposition is a pre-requisite for centromere formation and in turn kinetochore assembly, ensuring equal partitioning of genetic material between daughter cells during cell division.

Escort, deposition and eviction of the different histone variants depend on histone chaperones that play an important role in defining discrete chromatin landscapes important for genome function, stability and cell identity (Hammond *et al.*, 2017). These different histone chaperones, defined 'as factors that associate with histones and stimulate a reaction involving histone transfer without being part of the final product' (De Koning *et al.*, 2007), execute distinct functions in an interaction network, which has been extensively characterized in animals and yeast. Recently, 22 and 25 genes encoding histone chaperones in Arabidopsis and rice, respectively, have been identified (Tripathi *et al.*, 2015).

These proteins were classified into seven different families, namely NAP (NUCLEOSOME ASSEMBLY PROTEIN), CAF1 (CHROMATIN ASSEMBLY FACTOR 1), SPT6 (SUPPRESSOR OF TY ELEMENT 6), ASF1 (ANTI-SILENCING FACTOR 1), HIRA (HISTONE REGULATOR A), NASP (NUCLEAR AUTO-ANTIGENIC SPERM PROTEIN) and FACT (FACILITATES CHROMATIN TRANSCRIPTION). While some of these histone chaperones are known to specifically deposit a particular variant, such as H3.1 that is assembled by CAF-1 (Jiang and Berger, 2017; Benoit *et al.*, 2019), which histone chaperones store, escort and deposit the centromeric histone variant CenH3, initially termed HTR12 (Talbert *et al.*, 2002, 2012) in Arabidopsis, still remains unknown. In line with the low conservation of CenH3 proteins between species (Mattioli *et al.*, 2015), several distinct CenH3 chaperones have been identified. These include the Holliday junction recognition protein (HJURP) in humans (Dunleavy *et al.*, 2009; Foltz *et al.*, 2009), Scm3 in *Saccharomyces cerevisiae* and in *Schizosaccharomyces pombe* (Stoler *et al.*, 2007; Pidoux *et al.*, 2009), the fly-specific protein CAL1 in *Drosophila* (Phansalkar *et al.*, 2012; Chen *et al.*, 2014) and the Sim3 protein, a homolog of mammalian histone chaperone NASP, in *S. pombe* (Dunleavy *et al.*, 2007). HJURP specifically interacts with the pre-nucleosomal dimer CenH3–H4 (Dunleavy *et al.*, 2009; Foltz *et al.*, 2009; Mattioli *et al.*, 2015) and is required for *de novo* CenH3 deposition thereby also determining the position of novel centromeres (Barnhart *et al.*, 2011). Scm3 localizes to centromeres and is necessary for loading of CenH3 to the centromeres of *S. pombe* (Pidoux *et al.*, 2009), while Sim3 has been suggested to escort CenH3 proteins (Dunleavy *et al.*, 2007). Mammalian NASP has been initially identified as a linker histone chaperone (Richardson *et al.*, 2000) and was later detected in the cytosolic and nuclear ASF1 complex using mass spectrometry analysis or after biochemical fractionation (Jasencakova *et al.*, 2010; Apta-Smith *et al.*, 2018). It shuttles newly synthesized H3–H4 dimers in the cytosol from heat shock proteins (HSPs) to ASF1 (Campos *et al.*, 2010) and is involved in tending a reservoir of H3–H4 histones (Cook *et al.*, 2011). However, by immunostaining, NASP was mainly detected in the nucleoplasm (Apta-Smith *et al.*, 2018). Purified recombinant human sNASP promoted the assembly of nucleosomes containing H3 variants including CenH3^{CENP-A} (Osakabe *et al.*, 2010), but, *in vivo*, reducing NASP levels does not affect soluble CenH3 levels (Cook *et al.*, 2011), therefore a direct implication of mammalian NASP in CenH3 escort or deposition remains to be shown. Arabidopsis NASP^{SIM3} localizes to the nucleoplasm as observed for yeast Sim3 and mammalian NASP. It can bind monomeric H3.1 and H3.3 histones, while *in vitro* NASP^{SIM3} also interacts with H3.1–H4 or H3.3–H4 dimers (Maksimov *et al.*, 2016).

Here we identify NASP^{SIM3} as a binding partner of Arabidopsis CenH3. Highly expressed in actively dividing

tissues, with a similar pattern as CenH3, NASP^{SIM3} does not tightly interact with chromatin suggesting that it plays a role in escorting non-nucleosomal CenH3 histones. In line with this role, reducing NASP^{SIM3} expression negatively affects CenH3 deposition at centromeres.

RESULTS

NASP^{SIM3} binds CenH3

To screen for yet unknown interactors of Arabidopsis CenH3, we performed immunoprecipitation coupled to mass spectrometry. To this aim we used inflorescences of plants expressing CenH3 as an EYFP fusion (the genomic coding region of *CenH3* fused to the *EYFP* coding sequence) and precipitated gCenH3–EYFP with an anti-GFP antibody before submitting the co-immunoprecipitated proteins to mass spectrometry analysis. Plants expressing EYFP alone served as a negative control. In four independent gCenH3–EYFP mass spectrometry samples we identified between six and 14 peptides (coverage 15.65–35.57%) that corresponded to NASP^{SIM3} (AT4G37210) and which were not detected in the EYFP control samples (Figures 1a and S1a). Altogether 52 peptides matching NASP^{SIM3} with a combined coverage of 41.06% were detected, strongly suggesting that NASP^{SIM3} can be found in a complex with CenH3 *in vivo*. In an independent approach to identify CenH3 binding proteins, tandem affinity purification (TAP) experiments coupled to mass spectrometry analysis were performed using GSRhino–CenH3 and GSRhino–H3.1 proteins expressed under control of the 35S promoter in actively dividing Arabidopsis cell culture suspensions (Figure 1a and Supporting Information Figure S1a). In four independent pull down samples of both CenH3 and H3.1 eight to 10 peptides (coverage 20.9–26.6%) and nine or 10 peptides (coverage 20.1–30.1%), respectively, corresponding to NASP^{SIM3} have been identified (Figure S1b), while none was identified in the TAP assays with the GSRhino tag alone as bait. These results consolidate that CenH3 interacts *in vivo* with NASP^{SIM3}.

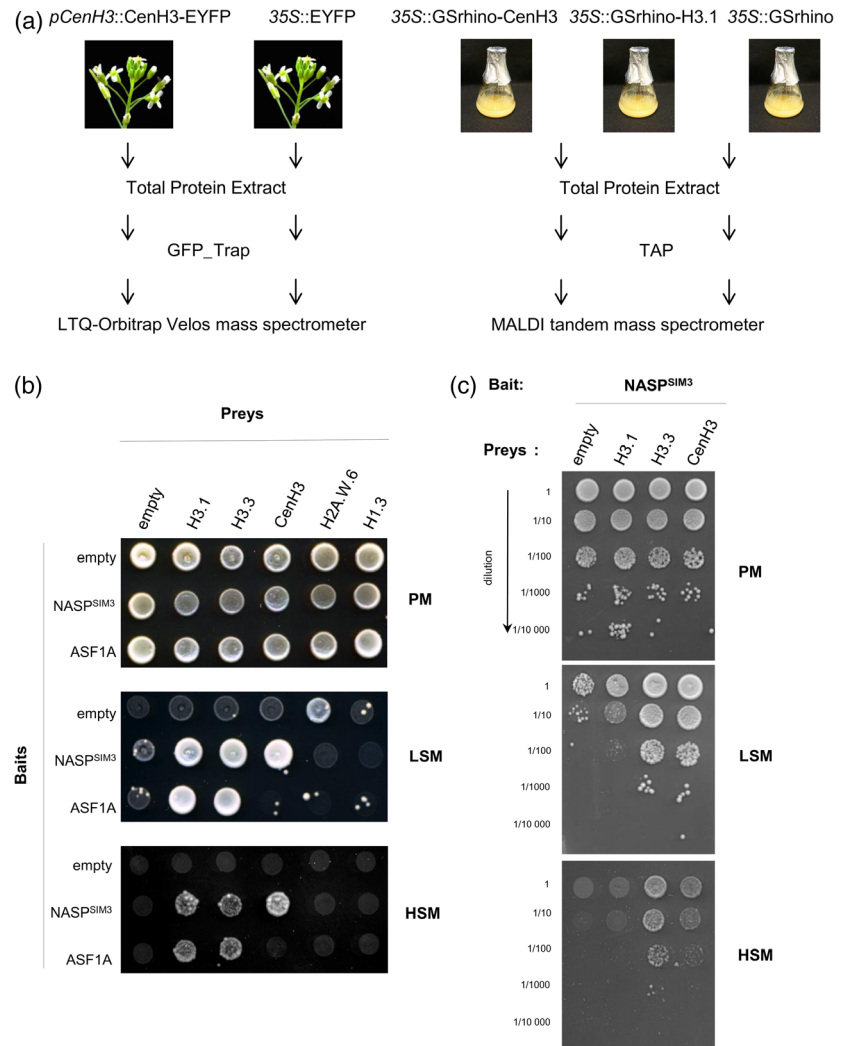
To determine whether NASP^{SIM3} interacts directly with CenH3 or is part of a complex including CenH3, we analyzed interactions of NASP^{SIM3} with different histone proteins using yeast-two-hybrid (Y2H) assay. Yeast strains expressing NASP^{SIM3} as bait, and H3.1, H3.3 or CenH3 as prey grew on selective medium, indicating that NASP^{SIM3} binds CenH3 (Figure 1b). CenH3 binding is specific to NASP^{SIM3} as the histone chaperone ASF1A, known in mammals to bind H3–H4 dimers (Natsume *et al.*, 2007), interacts with H3.1 and H3.3, but not with CenH3 (Figure 1a). Neither NASP^{SIM3} nor ASF1A-expressing strains grew on selective medium when co-expressed with an empty prey vector or with a vector expressing the H2A histone variant H2A.W.6 or the H1 variant H1.3 corroborating their specificity for H3 variants. A drop dilution test

Figure 1. Identification of NASP^{SIM3} as a CenH3 binding partner.

(a) Scheme illustrating the GFP-trap experiment using EYFP tagged CenH3 protein as bait and TAP experiments using GSRhino–CenH3 and GSRhino–H3.1. EYFP and GSRhino proteins were used as negative controls.

(b) Interaction between NASP^{SIM3} or ASF1A and the histone H3 variants H3.1, H3.3 and CenH3 or the histone variants H2A.W.6 and H1.3 as probed in a yeast-2-hybrid assay. Zygotes expressing both prey and bait are selected on PM (Permissive Medium: YNB without Leu and Trp). Protein–protein interactions are assessed on LSM (Low Stringency Medium: YNB without Leu, Trp and His) or HSM (High Stringency Medium: YNB without Leu, Trp, His and Ade).

(c) Strength of the protein–protein interactions between NASP^{SIM3} and H3.1, H3.3 or CenH3 was evaluated by drop dilution test.



revealed a strong interaction of NASP^{SIM3} with H3.3, followed by CenH3 and H3.1 (Figure 1c).

NASP^{SIM3} interacts with both C- and N-terminal parts of CenH3 *in planta*

To confirm the direct interaction between NASP^{SIM3} and CenH3 *in planta*, bimolecular fluorescence complementation (BiFC) assays were performed on young *Agrobacterium*-infiltrated tobacco (*Nicotiana benthamiana*) leaves (Walter *et al.*, 2004) containing mitotic cells. We first analyzed the nuclear distribution of NASP^{SIM3} and CenH3 proteins when transiently expressed in tobacco. Arabidopsis NASP^{SIM3} fused to EYFP localized to the nucleus, showing a uniform distribution excluding nucleoli (Figure 2a). When CenH3 was expressed with an N-terminal EYFP tag, two types of nuclei could be detected: either with an exclusive localization of the EYFP–CenH3 fusion protein in restricted spots corresponding to centromeres (Figure 2b) or both in the nucleoplasm and at centromeres (Figure 2c) showing that Arabidopsis CenH3 could be incorporated at

N. benthamiana centromeres under these conditions. When NASP^{SIM3} fused to the C- and CenH3 to the N-terminal YFP fragments, and *vice versa* were co-expressed in tobacco leaves, EYFP was successfully reconstituted in nuclei of the transformed cells with both combinations demonstrating interaction between NASP^{SIM3} and CenH3 *in planta* (Figure 2d,e). BiFC signals were diffuse throughout the nucleoplasm, and no specific enrichment was observed in defined spots.

We have shown previously that CenH3ΔN, lacking the N-terminal domain, localizes to centromeres (Lermontova *et al.*, 2006), indicating that the CenH3 histone fold domain is sufficient for its targeting to centromeres. Therefore, we tested which part of the CenH3 protein interacts with NASP^{SIM3}. To this end, the N-terminal tail (amino acids 1–70) or the histone fold domain (amino acids 71–178) of CenH3 were fused to the N- and C-terminal parts of YFP respectively, and co-expressed with full-length NASP^{SIM3}. BiFC signals could be detected in both cases (Figure 2f,g), showing that NASP^{SIM3} can interact both with the

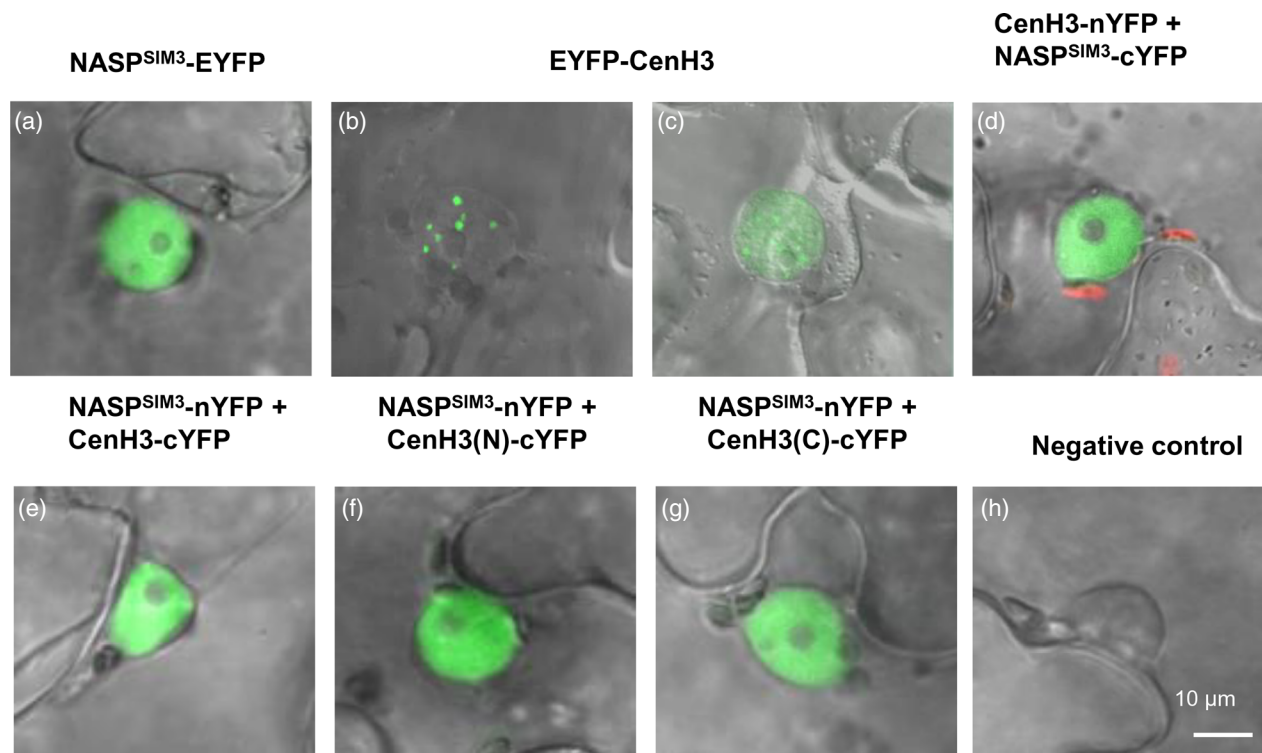


Figure 2. $NASP^{SIM3}$ binds both the N-terminal tail and the histone fold domain of CenH3 in planta.

(a–c) Localization of $NASP^{SIM3}$ -EYFP (a, green) and EYFP-CenH3 protein (b, c, green) in nuclei of *Nicotiana benthamiana* leaves.

(d, e) BiFC signals (green) revealing interaction of $NASP^{SIM3}$ with CenH3.

(f, g) BiFC signals revealing interaction of $NASP^{SIM3}$ with N- and C-terminal parts of CenH3, respectively.

(h) A representative example of negative control showing absence of BiFC signals. For the negative control experiments $NASP^{SIM3}$ -nYFP was co-injected with free cYFP and CenH3–cYFP with free nYFP.

N-terminal tail as well as independently with the histone fold domain of CenH3.

Control experiments, in which $NASP^{SIM3}$ -nYFP was co-expressed with free cYFP or CenH3-cYFP with free nYFP as well as combinations of N- and C-terminal parts of CenH3 fused with N- or C-terminal parts of EYFP, respectively, did not show any fluorescence excluding non-specific interactions of $NASP^{SIM3}$ or CenH3 with YFP (Figure 2h).

Arabidopsis $NASP^{SIM3}$ expressed in actively dividing tissues

Expression of Arabidopsis CenH3 is regulated by E2F, a transcription factor active in dividing tissues (Heckmann *et al.*, 2011). As the promoter of $NASP^{SIM3}$ contains a putative E2F binding site (Figure 3a) (Lermontova *et al.*, 2015), we speculated that it is expressed in dividing cells similar to CenH3.

To test whether Arabidopsis $NASP^{SIM3}$ is preferentially expressed and the corresponding protein is accumulated in dividing tissues, we generated transgenic lines expressing a $pNASP:NASP^{SIM3}$ -EGFP-GUS (for β -glucuronidase) reporter gene construct (Figure 3a), and analyzed the GUS staining pattern in these plants as a readout for $NASP^{SIM3}$ gene expression and protein accumulation. Although GUS

staining intensity varied between independent transgenic lines, all positive lines showed a similar staining pattern. Five representative lines were chosen for detailed analysis. In 4-day-old seedlings, GUS staining intensity was highest in root tips, shoot apical meristems and cotyledons (Figure 3b). In older plantlets (7-day-old, Figure 3c; 14-day-old, Figure 3d), $NASP^{SIM3}$ expression was also detected in young leaves containing actively dividing cells as previously reported (Maksimov *et al.*, 2016). In 4-week-old plants only young, but not old fully developed leaves showed GUS staining (Figure 3e–g). In inflorescence meristems, young inflorescences and developing flower buds GUS activity was almost absent (Figure 3h, upper part) or very weak (Figure 3h, lower part) but GFP signal from the $NASP^{SIM3}$ -EGFP-GUS fusion protein could be detected in petals of flower buds and in the developing male gametophyte (Figure S2a–d). However, older inflorescences displayed GUS activity of variable intensity in anthers and anther filaments (Figure 3h,i). Further data mining of some available RNA-seq datasets from different tissues and the eFP genome browser confirmed high $NASP^{SIM3}$ expression in tissues comprising dividing cells such as the root meristem and the shoot apex, but also found $NASP^{SIM3}$ transcripts to be abundant in flower buds

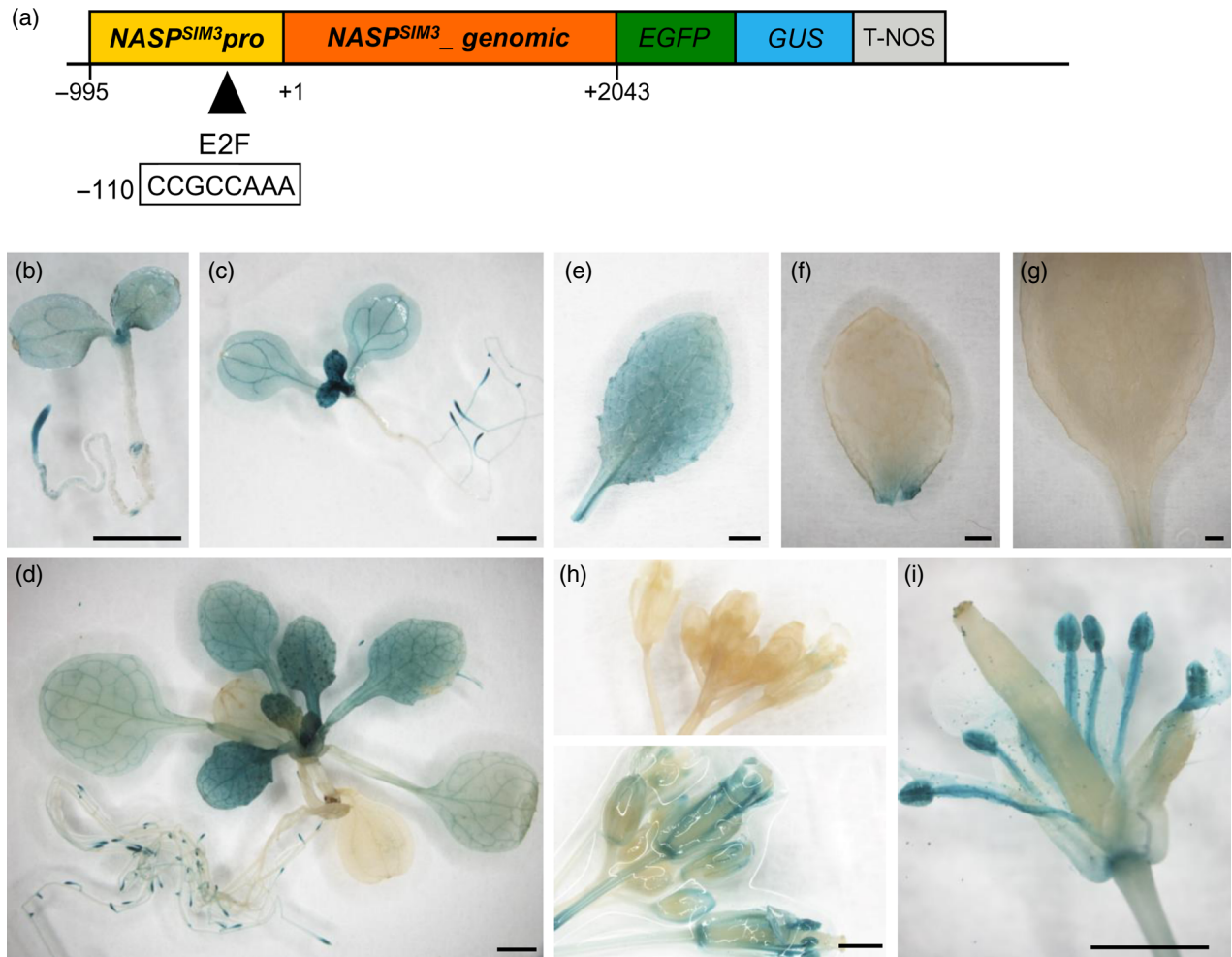


Figure 3. *NASP^{SIM3}* expression during development.

(a) Scheme of the *NASP^{SIM3}-EGFP-GUS* construct expressing *NASP^{SIM3}* as a translational fusion with EGFP and GUS under control of the endogenous promoter. The E2F binding site in the promoter is indicated.

(b–i) Histochemical localization of GUS activity in Arabidopsis plants transgenic for *NASP^{SIM3}-EGFP-GUS*: 4-day-old (a), 7-day-old (b) and 14-day-old (c) seedlings, rosette leaves of 4-week-old plants at different developmental stages (e–g), inflorescence (h), mature flower (i). Bars = 1 mm.

(Figure S2e,f), despite weak GUS staining. Similar to *NASP^{SIM3}*, *CenH3* shows highest expression in root and shoot meristems (Figure S2e,f).

Taken together, *NASP^{SIM3}* was preferentially expressed in dividing tissues similar to *CenH3*.

The predominant *NASP* isoform *NASP.1^{SIM3.1}* localizes to the nucleoplasm in the interphase

In different Arabidopsis databases, two different splice variants for the gene *At4g37210* are proposed; which differ in predicted amino acid sequence (Figures 4a left and S3a). Isoform *At4g37210.1* (*NASP.1^{SIM3.1}*) encodes for 492 amino acids and *At4g37210.2* for 378 amino acids (*NASP.2^{SIM3.2}*) lacking part of the C-terminal coiled-coil domain (Figure 4a, right) due to four nucleotides difference in length of exon 5, resulting in a frame shift generating a premature stop codon in exon 6. The corresponding cDNAs: CP002687.1 –

At4g37210.1 and NM_202970.1 – *At4g37210.2* were found in the Arabidopsis sequence database (<https://www.ncbi.nlm.nih.gov/>). To confirm the presence of both *NASP^{SIM3}* transcripts of Arabidopsis, we performed RT-PCR on RNA extracted from seedlings and flower buds with an isoform-specific reverse primer (Figure S3a,b). *At4g37210.1* transcripts could be detected in both seedlings and flower buds, while *At4g37210.2* transcripts were detected only in floral tissues (Figure S3b) confirming the existence of the short splice variant and suggesting tissue-specific expression.

To study the subcellular localization of the two predicted *NASP^{SIM3}* proteins we generated constructs expressing *NASP.1^{SIM3.1}* and *NASP.2^{SIM3.2}* cDNA fragments fused to EYFP under control of the CaMV 35S promoter. The two constructs were transiently expressed in leaves of *N. benthamiana* and for both *NASP^{SIM3}* isoforms EYFP fluorescence was observed in the nucleoplasm of epidermal

nuclei, whereas EYFP alone was localized in the nucleus and cytoplasm (Figure S3c). Both constructs were used to transform *A. thaliana* and the NASP.1^{SIM3.1}–EYFP fusion protein was localized in the nucleoplasm of root tip nuclei (Figure S3d), in agreement with previous reports (Maksimov *et al.*, 2016). In contrast, no transgenic plants could be recovered on selective media for the second, shorter isoform, in three independent transformation experiments. As expression of the NASP.2^{SIM3.2} isoform under the 35S promoter might result in overexpression and affect growth, genomic NASP.2^{SIM3.2} fragments including endogenous promoters were cloned to generate a translational fusion with GFP and GUS reporter genes as it was described above for the NASP.1^{SIM3.1} variant (Figure 3a). We showed that the longer isoform localizes to the nucleoplasm of root tip nuclei (Figure 4b,e) as previously reported (Maksimov *et al.*, 2016). For the shorter isoform, only a few transgenic lines showing GFP signals were obtained. Despite lacking part of the coiled-coil domain, the shorter isoform showed a similar nuclear localization to that of the longer isoform (Figure 4c). The weak expression of NASP.2^{SIM3.2} in our transgenic lines is in agreement with the mass

spectrometry experiments, in which no peptide was identified that could be specifically assigned to the NASP.2^{SIM3.2} isoform.

De novo incorporation of the CenH3 histone variant takes place during G2 phase of the mitotic cell cycle (Lermontova *et al.*, 2006, 2007). We therefore wanted to investigate whether the subcellular localization of the predominant, longer isoform NASP.1^{SIM3.1} would change during the mitotic cell cycle. The NASP.1^{SIM3.1}–GFP fusion is present as the same diffused nuclear stain in root tip meristems throughout G1, S and even in G2, when newly synthesized CenH3 is loaded (Figure 4e and Video S1). As during transient expression in *N. benthamiana* (Figure 2), we never observed a pronounced accumulation of NASP.1^{SIM3.1} next to chromocenters that could indicate a direct role of NASP.1^{SIM3.1} in CenH3 loading.

NASP^{SIM3} is highly mobile

To study the nuclear localization of Arabidopsis NASP.1^{SIM3.1} in relation to chromatin, we performed immunostaining with anti-GFP antibodies on nuclei of pNASP:NASP.1^{SIM3.1}–EGFP–GUS transformants and

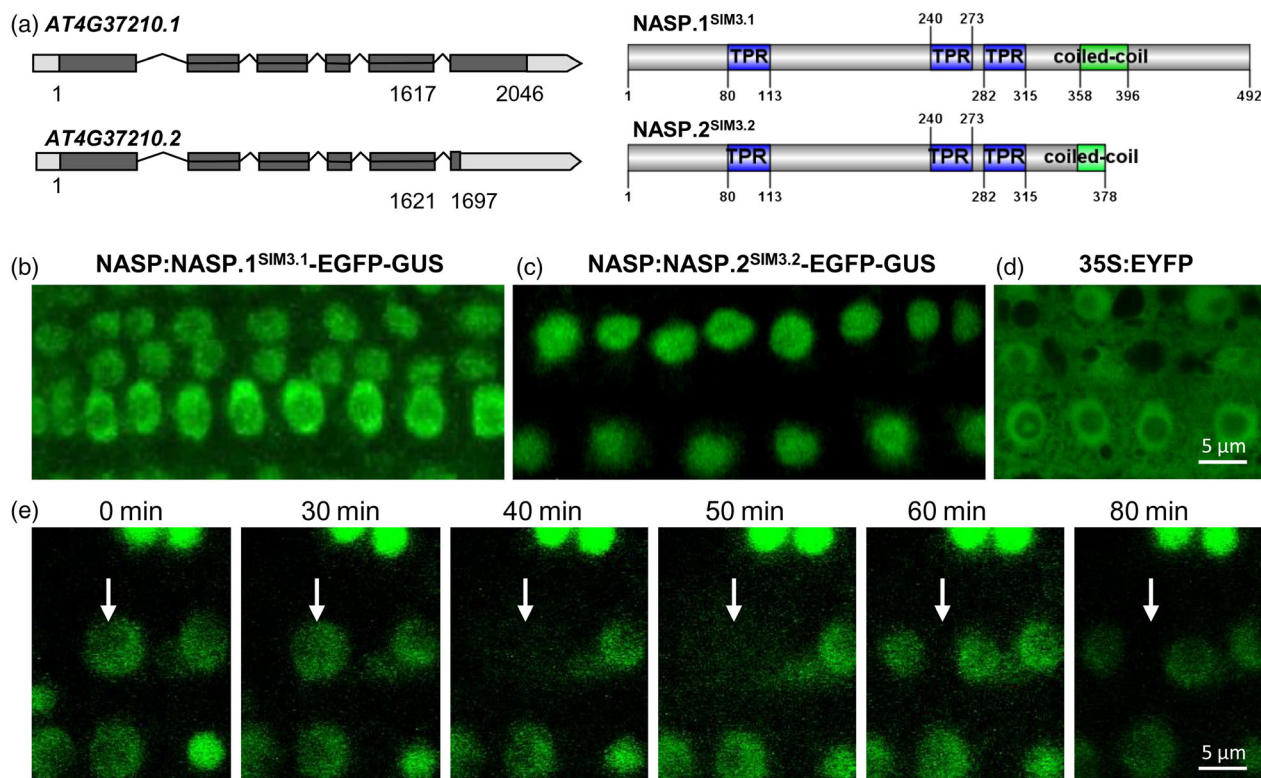


Figure 4. NASP^{SIM3} localizes to the nucleoplasm of Arabidopsis root tip nuclei.

(a) Schematic view of the gene structure of NASP^{SIM3} splice variants and corresponding protein isoforms. The shorter transcript variant is formed due to alternative splicing (four nucleotide longer exon 5) resulting in a frame shift and premature stop codon in exon 6. The resulting protein isoform lacks part of the coiled-coil domain. Graphical scheme of domains was prepared in DOG 1.0 (Domain Graph; Ren *et al.*, 2009). (b–d) Root tip of *Arabidopsis thaliana* expressing the NASP:NASP.1^{SIM3.1}–EGFP–GUS (b) NASP:NASP.2^{SIM3.2}–EGFP–GUS (c) and 35S:EYFP (d) constructs. Both NASP.1^{SIM3.1}–EGFP–GUS (b) and NASP.2^{SIM3.2}–EGFP–GUS (c) fusion proteins showed nuclear localization, while EYFP alone (d) was detected in nuclei and cytoplasm. (e) Live imaging of root tip cells of Arabidopsis transformed with the NASP:NASP.1^{SIM3.1}–EGFP–GUS fusion construct. The arrow indicates a cell undergoing mitosis.

applied structured illumination microscopy. At this higher resolution, NASP.1^{SIM3.1} partly co-localizes with chromatin fibers, but is excluded from chromocenters and the nucleolus (Figure 5a). However, it does not completely follow the chromatin pattern and also occurs in between chromatin fibers. Super-resolution microscopy indicates that the NASP.1^{SIM3.1}-EGFP-GUS fusion protein is not associated with mitotic chromosomes (Figure 5b).

To further test whether Arabidopsis NASP.1^{SIM3.1} was associated with chromatin, we used BY-2 cells expressing CenH3-EGFP and NASP.1^{SIM3.1}-mCherry. In these highly dividing cells, CenH3-EGFP localized to centromeres and NASP.1^{SIM3.1}-mCherry showed a diffuse nuclear staining coherent with our previous observations (Figure S4). When we permeabilized these cells using detergent to release non-chromatin bound proteins from the nucleus, CenH3-EGFP signal was still distinctly detectable in the nucleus and mostly at centromeres (Figure S4), while the NASP.1^{SIM3.1}-mCherry signal was visibly reduced compared to the non-treated condition. This indicates that most of the NASP^{SIM3} proteins were part of the soluble nuclear protein pool and did not stably associate with chromatin. To confirm this observation with a different assay, we probed the dynamics of NASP.1^{SIM3.1} by fluorescence recovery after photobleaching (FRAP) and fluorescence loss in photobleaching (FLIP) (Figure 5c–f). The unique bleaching of a distinct nuclear area in roots of plants expressing genomic NASP.1^{SIM3.1} fragments in fusion with EGFP showed almost complete signal recovery within 35 sec (Figure 5c,f). In an experiment with repeated bleaching (every 5 sec) of a selected area (Figure 5d,f) the fluorescence was partially recovered in about 2 sec after each bleaching step. In FLIP experiments, based on the constant bleaching of a distinct area of the nucleoplasm, the NASP.1^{SIM3.1}-EGFP-GUS fluorescence was completely bleached within 30 sec (Figure 5e,f). In short, FRAP and FLIP experiments revealed a high turnover and mobility of the NASP.1^{SIM3.1} protein and confirmed that NASP.1^{SIM3.1} was not tightly associated with chromatin.

NASP^{SIM3} interaction network

To identify other binding factors of Arabidopsis NASP^{SIM3} that may reinforce its role as CenH3 chaperone, we carried out a Y2H screen using the long NASP.1^{SIM3.1} isoform as bait. Among the putative binding partners of NASP.1^{SIM3.1} we identified three candidates with a clear link to chromatin: the histone variant H3.3, the WD40 repeat-containing protein MSI3 as well as the H2A–H2B histone chaperone NAP1;2 (NUCLEOSOME ASSEMBLY PROTEIN 1) (Liu *et al.*, 2009). MSI3 is a homolog of MSI1, which is a subunit of the CHROMATIN ASSEMBLY FACTOR 1 (CAF-1) complex and which has previously been identified by immunoaffinity purification of YFP-tagged NASP^{SIM3} (Maksimov *et al.*, 2016) (Figure 6a). We further identified TSK-

ASSOCIATING PROTEIN (TSA1) (Suzuki *et al.*, 2005) that had been previously shown to bind to Gamma-tubulin Complex Protein 3- interacting proteins (GIPs) that in turn also interacted with CenH3 (Janski *et al.*, 2012; Batzenschlager *et al.*, 2013). This therefore suggests an additional link with the centromere. To validate the interaction of NASP^{SIM3} with NAP1;2 and TSA1, we cloned the corresponding full-length cDNAs and confirmed that NASP^{SIM3}, but not ASF1, interacted both with NAP1;2 and TSA1, while the interaction was stronger with NAP1;2 (Figure 6b,c).

NASP^{SIM3} knockdown impairs CenH3 deposition

To test whether NASP^{SIM3} is important to maintain CenH3 levels or its deposition, we aimed to analyze NASP^{SIM3} loss of function phenotypes. As T-DNA insertion lines are not available we turned to existing RNAi lines (Maksimov *et al.*, 2016) and generated transgenic lines expressing an artificial miRNA construct directed against NASP^{SIM3}. We identified few lines with reduced NASP^{SIM3} mRNA levels, out of which we selected two lines (RNAi line 4 and amiRNA line 22) for further analysis (Figure 7a). These plants did not show any obvious phenotypic abnormalities during vegetative growth, but demonstrated slightly reduced seed setting and an increased number of aborted seeds (Figure S5).

To investigate whether reduced NASP^{SIM3} expression would affect nuclear CenH3 levels and its deposition, we determined CenH3 levels relative to H4 in nuclear extracts of 10-day-old plantlets from two independent wild-type seed batches and the two transgenic lines with reduced NASP^{SIM3} expression. We reproducibly found a moderate but significant reduction of nuclear CenH3 levels in these two lines compared to the wild-type (WT) (Figure 7b,c). To investigate whether this reflected global CenH3 levels or might also impact nucleosomal CenH3 at centromeres, we sorted 4C nuclei isolated from 3-day-old seedlings of the RNAi line 4 and wild-type plants and carried out immunostaining with anti-CenH3 antibodies. Fluorescence image stacks of each genotype were acquired using structured illumination microscopy and the sum of the fluorescence intensities from the centromere (CenH3) signals was calculated. The level of CenH3 at the centromeres of the NASP^{SIM3} RNAi line was reduced ~30% compared with the wild-type (Figure 7d,e).

Taken together, these results indicated that reduced NASP^{SIM3} expression negatively affects CenH3 levels. We assumed that reduced loading of CenH3 in plant lines with lower NASP^{SIM3} levels might result in generation of haploids in crosses with wild-type plants as it was described for plants with altered expression of CenH3 (Ravi and Chan, 2010). To test this hypothesis, the RNAi line 4 was crossed with wild-type. The ploidy level of nuclei from 105 F1 seeds was analyzed by flow cytometry, however, all nuclei were found to be diploid (Figure S6).

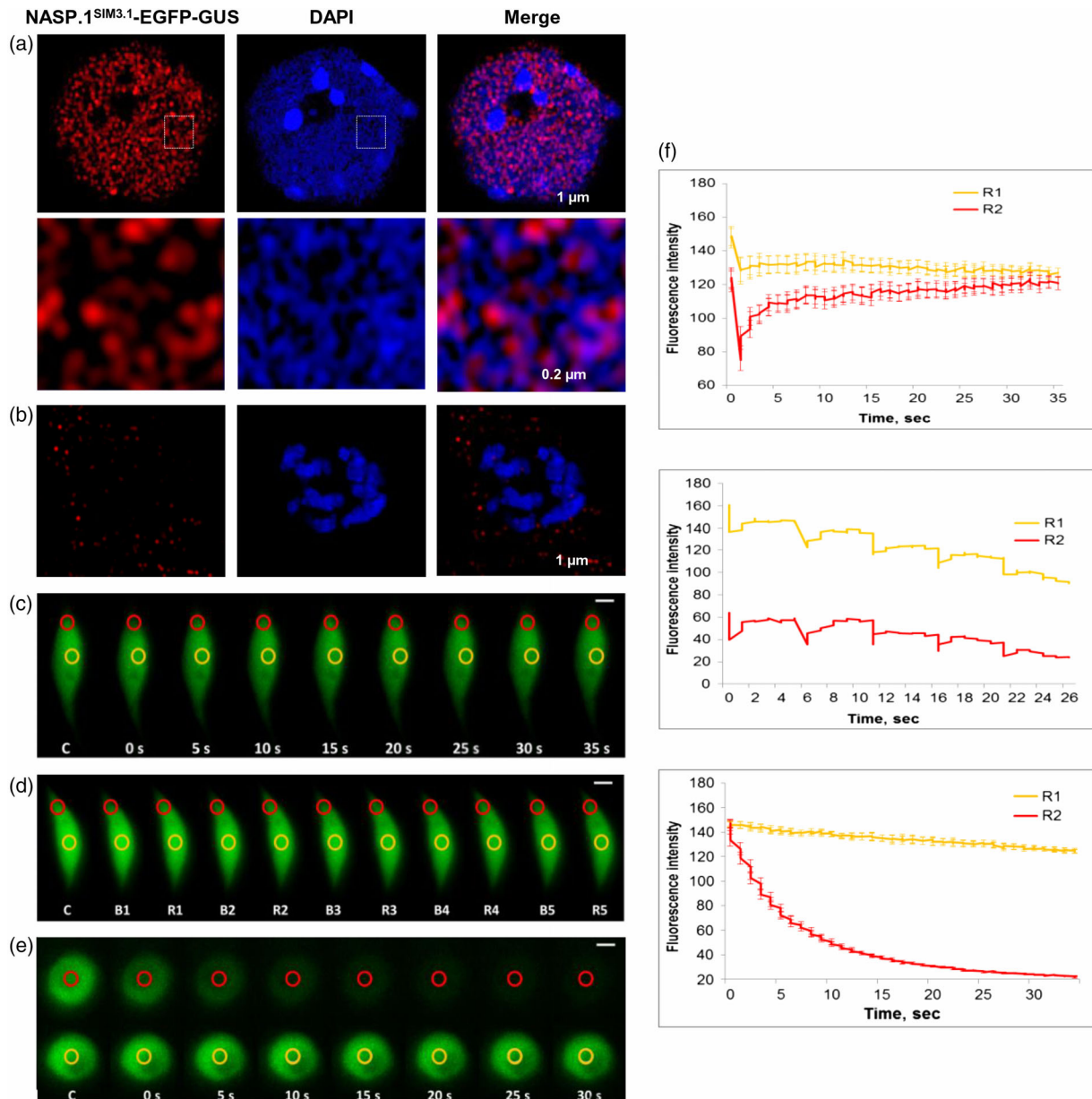


Figure 5. NASP.1^{SIM3.1} protein is highly dynamic and does not stably associate with chromatin.

(a) Upper panel: Nucleus of a NASP.1^{SIM3.1}-EGFP-GUS transformed Arabidopsis plant immunostained with anti-GFP antibodies (red) imaged with structural illumination microscopy. NASP.1^{SIM3.1}-EGFP immunosignals are localized to the nucleoplasm and absent from DAPI-bright chromocenters (blue). Lower panel: The images show enlarged regions delimited by dashed boxes in the upper panel.

(b) Cell of an NASP.1^{SIM3.1}-EGFP-GUS transformed Arabidopsis plant immunostained with anti-GFP antibodies (red) revealing absence of NASP.1^{SIM3.1} immunosignals from mitotic chromosomes.

(c) Single FRAP in a differentiated root nucleus. A small circular area (1.5 μm in diameter) in the root periphery (red circle) was bleached for 350 μsec and let recover for 35 sec. The yellow circle indicated the non-bleached area of the nucleus imaged for comparison. C = control pre-bleach fluorescence.

(d) Repeated FRAP in a differentiated root nucleus. A small area (1.5 μm in diameter) in the root periphery (red circle) was repeatedly bleached (B1–B5) for 250 μsec followed by 5 sec recovery (R1–R5). Fluorescence in the non-bleached area of the nucleus (yellow circle) declines as unbleached molecules diffuse into the bleached area. C = control pre-bleach fluorescence.

(e) Fluorescence loss in photobleaching (FLIP) measurements in a root nucleus in the meristematic zone. Small central area (1.5 μm in diameter) of a root tip nucleus was repetitively bleached for 50 μsec with 300 μsec interval. Fluorescence in the bleached area (red circle) and the non-bleached control area (yellow circle) were followed for 30 sec. In all images: Bar = 2 μm.

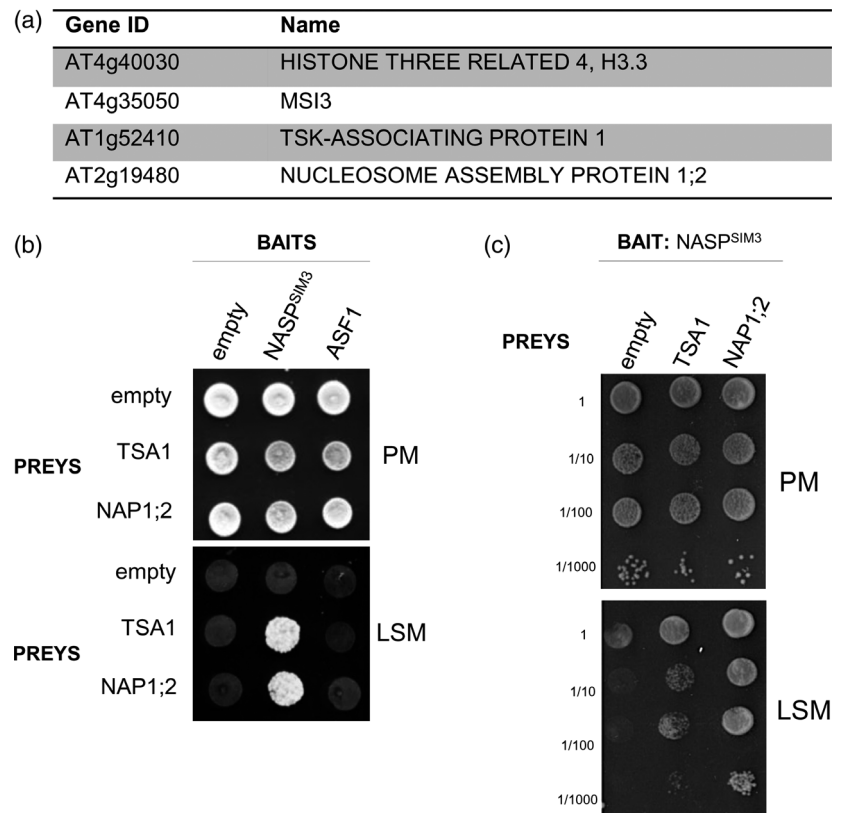
(f) Graphs show average values of relative fluorescence intensity from five independent experiments. Upper graph: corresponds to the single FRAP (c), middle graph: corresponds to the repeated FRAP (d) and lower graph: corresponds to FLIP (e). R1 – unbleached area (yellow circle), R2 – bleached area (red circle).

Figure 6. NASP^{SIM3} interaction network.

(a) Preys identified in a yeast-two-hybrid screen using NASP.1^{SIM3.1} as bait.

(b) Interaction between NASP.1^{SIM3.1} or ASF1A and TSA1 and NAP1;2. Zygotes expressing both bait and prey are selected on PM (Permissive Medium: YNB without Leu and Trp). Interactions are assessed on LSM (Low Stringency Medium: YNB without Leu, Trp and His).

(c) The strength of the protein–protein interaction between NASP^{SIM3} and TSA1 or NAP1;2 was evaluated by drop dilution test.



DISCUSSION

The chromosomal location where kinetochores assemble during mitosis and meiosis is in most organisms not defined by DNA sequence but by a specific chromatin organization demarcated by incorporation of the histone variant CenH3. Controlled storage and transport of CenH3 histones, as well as its deposition only at specific genomic locations, are therefore critically important for the balanced segregation of the chromosomes to daughter cells (Lacoste *et al.*, 2014; Müller and Almouzni, 2017). Despite its conserved function in eukaryotes, CenH3 molecules are highly divergent between species. In particular the N-terminus of CenH3, longer than that of H3.1 or H3.3, shows variability in length and sequence composition between different phylogenetic groups and even within a genus such as *Drosophila* (Rosin and Mellone, 2017). In Arabidopsis the N-terminus of CenH3 is required for CenH3 loading to centromeres of meiotic, but not of mitotic chromosomes (Lermontova *et al.*, 2011; Ravi *et al.*, 2011). It was suggested that in the absence of the N-terminus, which may be involved in protein–protein interaction like its homolog in yeast (Chen *et al.*, 2000), CenH3 cannot be recognized by meiosis-specific chaperones, and therefore cannot be loaded onto centromeres. At present, the existence of mitosis and meiosis-specific mechanisms of CenH3 loading to centromeres remains unanswered. In metazoans structurally different protein complexes are involved in CenH3 deposition such as HJURP

in humans and CAL1 in *Drosophila*, but no CenH3 transport or deposition factor had so far been identified in plants.

NASP^{SIM3} – histone interaction

By searching for Arabidopsis CenH3 interactors in two independent experimental setups, we identified NASP^{SIM3} as an *in vivo* CenH3 binding partner and confirmed interaction between NASP^{SIM3} and CenH3 using two independent approaches such as Y2H assays and BiFC. NASP^{SIM3} is an evolutionary highly conserved protein that was likely to be already present in the first eukaryotic ancestor (Nabeel-Shah *et al.*, 2014). NASP^{SIM3} comprises three canonical tetratricopeptide repeat (TPR) motifs and a putative TPR motif interrupted by a large acidic region in its N-terminus and a predicted coiled-coil domain in its C-terminus. Arabidopsis NASP^{SIM3} has previously been shown to bind with similar affinity to both H3.1 and H3.3 (Maksimov *et al.*, 2016) likely through a conserved heptapeptide motif LA-IRG in the C-terminal region of histone H3 that is sufficient for the interaction with the TPR motifs of human and Arabidopsis NASP^{SIM3} (Bowman *et al.*, 2016). This heptapeptide is highly conserved in different H3 variants including human CenH3^{CENP-A}, therefore suggesting that the interaction between Arabidopsis NASP^{SIM3} and CenH3 would take place via the CenH3 HFD domain. However, while the LA-IRG motif is conserved in Arabidopsis H3.1 and H3.3, this motif differs in Arabidopsis CenH3 (namely LA-LGG). This

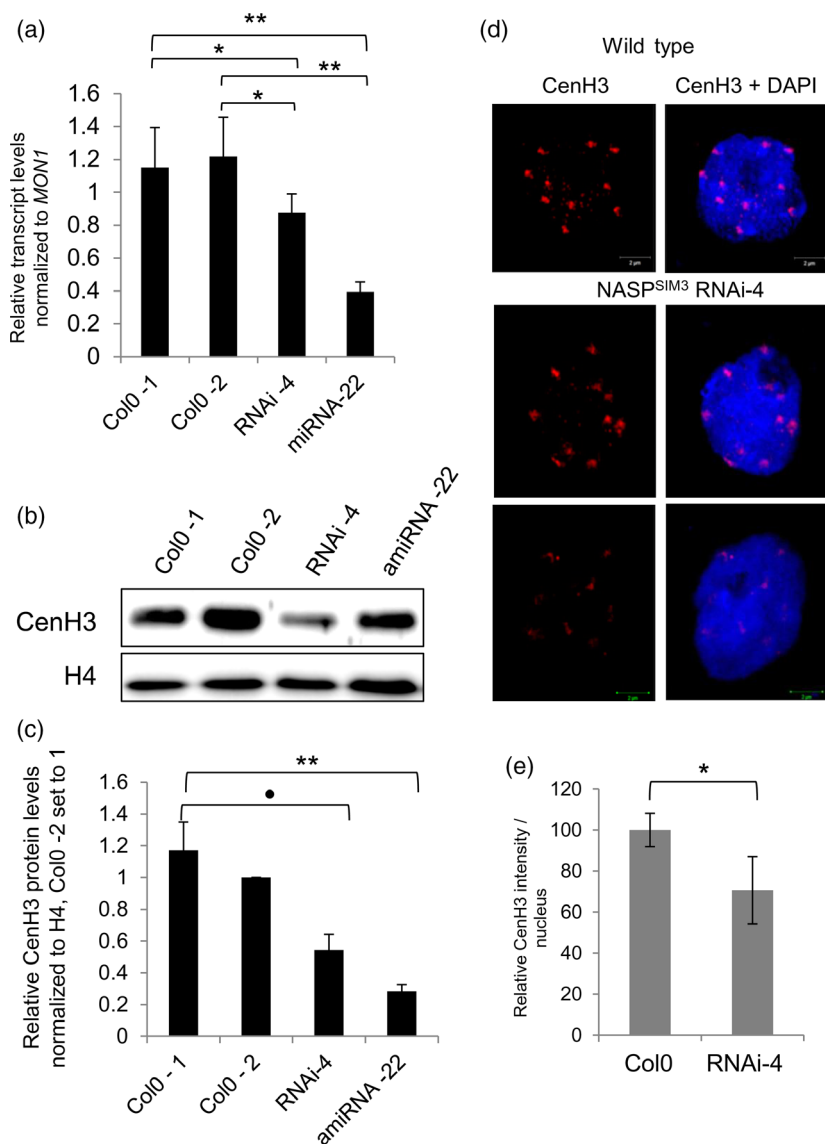


Figure 7. Reduced NASP^{SIM3} levels affect CenH3 deposition.

(a) NASP^{SIM3} transcript levels in seedling from two independent wild-type (WT) (Col 0) seed batches, a line expressing an RNAi construct (RNAi-4) or an artificial miRNA (amiRNA-22) directed against NASP^{SIM3} transcripts. Relative NASP^{SIM3} transcript levels normalized to *MON1* are shown, one sample of the three biological replicates of Col0 seed batch 2 was set to 1.

(b) CenH3 protein levels in nuclear extracts from seedlings revealed by western blotting using an anti-CenH3 antibody. CenH3 levels were normalized to H4 levels.

(c) Quantification of CenH3 band intensities relative to H4 from at least three independent biological replicates. Relative CenH3 levels in seedling from the Col0 seed batch 2 were set to one in each independent experiment. Error bars correspond to SEM. Student's *t*-test, ***P* < 0.01; **P* < 0.05; •*P* < 0.07.

(d) Representative nuclei isolated from 3-day-old WT nuclei and the NASP^{SIM3} RNAi line 4 (RNAi-4). Endogenous CenH3 was revealed by immunostaining with anti-CenH3 antibodies.

(e) Quantification of relative intensity of CenH3 immunosignals at centromeres of wild-type and NASP^{SIM3} RNAi-4. *n* (WT) = 10; *n* (RNAi-4) = 14. Error bars correspond to SEM. Mann-Whitney Rank Sum Test: **P* < 0.05.

therefore suggests the existence of additional contacts between CenH3 and NASP^{SIM3}. Indeed, while interaction of NASP with the H3 C-terminus was lost in a human sNASP binding mutant, this did not completely abolish binding to full-length H3 (Bowman *et al.*, 2016) and in our BiFC assays NASP^{SIM3} interacts both with the HFD of CenH3 and its N-terminus. A possible supplementary interaction motif could be the proline-rich GRANT motif recently defined in the fission yeast CenH3 N-terminus that is required for interaction with Sim3 (Tan *et al.*, 2018). However, our analysis of the N-termini of different plant CenH3 proteins did not reveal a conserved GRANT motif in plants, suggesting yet another mode and domain of interaction between Arabidopsis CenH3 and NASP^{SIM3}. Such multivalent protein-protein interactions between histones and chaperone proteins as observed for NASP^{SIM3} and CenH3 might allow

handing over CenH3 to other transport or assembly factors or histone modifiers. Alternatively, it may reflect different binding modes of CenH3 to either monomeric CenH3 or CenH3-H4 dimers. Despite the fact that it was reported that the mammalian NASP forms also complexes with H1 linker histones through the acidic patch present in TPR2, which is conserved in Arabidopsis NASP^{SIM3} (Richardson *et al.*, 2000; Cook *et al.*, 2011; Wang *et al.*, 2012), we did not find evidence that Arabidopsis NASP^{SIM3} binds H1 or H2A histones implying specificity for H3 histones.

CenH3 is predominantly expressed in cells that are actively dividing, an expression pattern that can be explained by specific binding sites for the E2F transcription factor in its promoter (Heckmann *et al.*, 2011). We find that the NASP^{SIM3} promoter also contains an E2F binding site. Accordingly, NASP^{SIM3} shows elevated

promoter activity and transcript levels in dividing cells such as shoot and root meristems, similar to mammalian NASP that parallels histone expression (Richardson *et al.*, 2000). For most tissues, NASP^{SIM3} transcript levels were also reflected at the level of the NASP^{SIM3}-EGFP-GUS fusion protein except for young flower buds, which showed weak GUS staining (Figure 3h) and revealed low GFP fluorescence in petals and the developing male gametophyte (Figure S2a–d). This observation is potentially echoing the weak correlation between transcript and protein levels as frequently observed (Jiang *et al.*, 2007; Nakaminami *et al.*, 2014).

Nevertheless, the high expression in root meristems for example, points to a role in escorting CenH3, while not excluding a role for NASP^{SIM3} in chaperoning H3 variants during DNA replication when histone pools are particularly dynamic. Indeed, a recent study indicated that the inheritance of pre-existing CenH3^{CENP-A} nucleosomes at the replication fork requires dedicated machinery that differs from H3.1 and H3.3 maintenance and involves HJURP recruitment (Zasadzińska *et al.*, 2018).

NASP^{SIM3} splice variants

In most vertebrate species, functional diversity of NASP proteins is generated through different splice variants. In mammals, alternative splicing generates two different isoforms, tNASP, highly expressed in testis, and sNASP that is rather ubiquitously expressed (Richardson *et al.*, 2000). In Arabidopsis, there is evidence for expression of a shorter NASP.2^{SIM3.2} isoform with a truncated coiled-coil domain. While absent from most RNA-seq datasets, suggesting low abundance, we confirmed the presence of this alternative transcript in flower buds and showed that the corresponding protein as a GFP fusion was weakly expressed with similar nuclear localization than the longer isoform. BLAST search against NASP.1^{SIM3.1} cDNA of Arabidopsis revealed two splicing variants in cotton *Gossypium raimondii*: XP 012491717.1, corresponding to the longer isoform, and XP 012491718.1, corresponding to the shorter isoform, while in other plant species only the NASP.1^{SIM3.1} variant could be identified. It is very likely that the NASP.2^{SIM3.2} isoform is not represented in transcriptomes of most species due to its low abundance and limitations of the transcriptome assembly algorithms.

If a NASP^{SIM3} knock-out were available, it would be interesting to investigate whether the short isoform complements the mutant phenotypes or whether a functional coiled-coil domain is essential for NASP^{SIM3} function, e.g. by mediating critically important protein–protein interactions essential for H3 or CenH3 handling. The fact that we never recovered plant lines with the 35S::NASP.2^{SIM3.2} - GFP construct that might function as a dominant negative may point in this direction.

Impact of reduced NASP^{SIM3} expression

In contrast with mammals or *Drosophila*, in which loss of histone chaperones such as CAF-1, HIRA, ASF-1 and NASP causes early embryonic lethality, Arabidopsis plants lacking CAF-1, HIRA and both ASF-1 orthologues are viable (Kaya *et al.*, 2001; Zhu *et al.*, 2011; Duc *et al.*, 2015) indicating an important plasticity in histone handling in plants. Because we did not find lines with strongly reduced NASP^{SIM3} expression and several attempts to generate *nasp* mutant plants with CRISPR-Cas9 technology have been unsuccessful, NASP^{SIM3} is likely to play an essential role in histone H3 handling in plants. Whether CenH3 could be bound by other factors such as the FACT complex (Okada *et al.*, 2006) remains to be determined.

NASP^{SIM3} interaction network

Previous studies have shown that NASP^{SIM3} interacts with the heat shock 70 kDa protein HSC70-1 and the WD-40 repeat-containing protein MSI1 (Maksimov *et al.*, 2016), the latter being one of the three subunits of the CAF-1 complex as well as of various remodeling complexes (Kaya *et al.*, 2001; Hennig *et al.*, 2005). By screening an Y2H library we have identified here MSI3 as an additional NASP^{SIM3} binding partner. MSI proteins are conserved histone binding proteins that bind non-nucleosomal histones H4. Interaction with NASP^{SIM3} could therefore be direct or occur via histones. Our screen further revealed interaction with histones as expected and with one of the four NAP homologs NAP1;2, a H2A-H2B chaperone. While predominantly cytoplasmic, a small fraction of NAP1;2 was found as well in the nucleus and shown to bind chromatin (Liu *et al.*, 2009). Finally, we detected interaction with TSA-associated protein 1 (TSA1) that is preferentially expressed in shoot apices similar to NASP^{SIM3} (Suzuki *et al.*, 2005) and localizes in ER body-like structures and at the nuclear envelope (Batzenschlager *et al.*, 2013) where centromeres are preferentially localized (Fang and Spector, 2005). TSA1 interacts with the small GIP proteins, which also bind CenH3. Similar to NASP^{SIM3}, loss of GIP proteins results in reduced CenH3 loading (Batzenschlager *et al.*, 2015), establishing an additional indirect link of NASP^{SIM3} in centromere function. While NASP^{SIM3} is detected predominantly in the nucleus in interphase, the interaction with two proteins (NAP1;2 and TSA1), which are reported to be predominantly cytoplasmic, could also indicate existence of a small cytoplasmic fraction of NASP^{SIM3} in plant cells.

Role of NASP^{SIM3} in CenH3 escort

Reduced NASP^{SIM3} expression affected CenH3 levels and deposition that, however, had no effect on chromosome segregation and did not lead to the generation of haploids in crosses with wild-type (Figure S6) as it was described for the *cenh3* mutant complemented by a GFP tagged

version of CenH3, in which the N-terminal tail was replaced by the one from histone H3.3 (Ravi and Chan, 2010). This could be explained by the fact that only plants with weakly affected *NASP^{SIM3}* expression and in consequence only ~30% reduced CenH3 levels were obtained. While we cannot exclude a more direct role for *NASP^{SIM3}* in CenH3 deposition or inheritance at the replication fork, most of our evidence points to a role in CenH3 escort like its yeast homolog (Dunleavy *et al.*, 2007). Confocal or high-resolution imaging of independent *NASP^{SIM3}*–GFP, *NASP^{SIM3}*–EGFP–GUS and *NASP^{SIM3}*–mCherry fusions showed a diffuse nuclear staining excluding nucleoli, coherent with previous observations (Maksimov *et al.*, 2016) and in agreement with a role for *NASP^{SIM3}* in chaperoning not only CenH3 but also H3.1 and H3.3. FRAP analysis together with the loss of nuclear *NASP^{SIM3}* by detergent extraction further revealed that the majority of Arabidopsis *NASP^{SIM3}* is not tightly associated with chromatin. In addition, no enrichment of BiFC signals was observed at centromeres, which may have indicated *NASP^{SIM3}*–CenH3 interaction during CenH3 deposition, despite the correct loading of CenH3 in these actively dividing cells. It is therefore likely that *NASP^{SIM3}* is not directly involved in CenH3 deposition, but rather binds CenH3 in its soluble, not chromatin bound, state. This is in agreement with the fact that in mammalian cells *NASP* depletion mostly affects the soluble H3–H4 pool and the observations that Arabidopsis *NASP^{SIM3}* preferentially binds to monomeric H3.1 and H3.3 *in vivo* (Maksimov *et al.*, 2016). *NASP^{SIM3}* may thereby ensure CenH3 supply by maintaining the nuclear CenH3 pool and escort CenH3 to the corresponding assembly factor as suggested for Sim3 (Dunleavy *et al.*, 2007). Further identification of additional *NASP^{SIM3}* binding partners, may allow us to determine the factors or complexes to which *NASP^{SIM3}* hands over CenH3 histones for chromatin assembly.

EXPERIMENTAL PROCEDURES

Plasmid construction and plant transformation

In detail, to generate CenH3–EYFP expressing plants, EYFP CDS (without START/STOP codon; flanked 5' and 3' with short neutral linker sequences) was amplified using primer TAG_cloning_for and TAG_cloning_rev (Table S1), cloned in vector pCRTM–Blunt (Invitrogen, <http://www.thermofisher.com/invitrogen>) generating pBlunt–EYFP–TAG, and confirmed by sequencing. EYFP CDS was then amplified from pBlunt–EYFP–TAG using primer GFPs_CDScloning_for and GFPs_CDScloning_rev (Table S1) and cloned via *SpeI/SalI* in the p35S–Nos–BM vector (<http://www.dna-cloning.com>). The resulting expression cassette (35S promoter, EYFP CDS, Nos terminator) was subcloned via *SfiI* into the binary vector pLH7000 (<http://www.dna-cloning.com>).

To generate gCenH3–EYFP expressing plants, the *CenH3* genomic locus was amplified using primer P1_CenH3 and P2_CenH3 as well as P3_CenH3 and P4_CenH3 (Table S1). Using primer TAG_for and TAG_rev (Table S1), EYFP CDS was amplified from

pBlunt–EYFP–TAG. The three resulting amplicons were merged into one product in a subsequent PCR reaction using primer P1_universal_TT and P2_universal_TT (Table S1), inserted via *SfiI* in vector p35S–Nos–BM ([dna-cloning-service.com](http://www.dna-cloning.com)), and confirmed by sequencing. Resulting expression cassette (CenH3 genomic locus expressing CenH3 internally in frame fused via linker sequences with EYFP) was subcloned via *SfiI* into pLH7000 (<http://www.dna-cloning.com>).

To study the localization of *NASP.1^{SIM3.1}* and *NASP.2^{SIM3.2}* *in vivo*, entire open reading frames were amplified by RT-PCR from RNA isolated from flower buds of *A. thaliana* Col-0 plants using *NASP^{SIM3}*_cDNA_f and *NASP.1^{SIM3.1}*_cDNA_r or *NASP^{SIM3}*_cDNA_f and *NASP.2^{SIM3.2}*_cDNA_r primers (Table S1), respectively and cloned into the pDONR221 vector (Invitrogen, <https://www.thermofisher.com/invitrogen>) via the Gateway BP reaction. From pDONR221 clones, cDNA fragments were recombined via Gateway LR reaction (Invitrogen, <https://www.thermofisher.com/invitrogen>) into the two attR recombination sites of the Gateway-compatible vectors pGWB41 and pGWB42 (<http://shimane-u.org/nakagawa/gbv.htm>), respectively.

To study the activity of the *NASP^{SIM3}* promoter in different *A. thaliana* tissues, and to identify the localization pattern of *NASP^{SIM3}* proteins expressed under the native promoter, genomic *NASP.1^{SIM3.1}* (–995 up to +2043 relative to the transcriptional *NASP^{SIM3}* start site) and *NASP.2^{SIM3.2}* (–995 up to +1694 relative to the transcriptional *NASP^{SIM3}* start site) fragments were amplified by PCR from Col-0 genomic DNA using *NASP^{SIM3}*_promoter_f and *NASP.1^{SIM3.1}*_genomic_r or *NASP^{SIM3}*_promoter_f and *NASP.2^{SIM3.2}*_genomic_r primers (Table S1), respectively and cloned into the pDONR221 vector. These constructs were used to generate *NASP^{SIM3}*_gen:EGFP–GUS reporter constructs using the pKGWFS7.0 vector (<http://gateway.psb.ugent.be/information>).

To generate plants with reduced *NASP^{SIM3}* levels, artificial miRNAs were designed with the web microRNA designer WMD3 tool (Ossowski Stephan, Fitz Joffrey, Schwab Rebecca, Riester Markus and Weigel Detlef, personal communication) and cloned into pRS300 (Schwab *et al.*, 2006) with subsequent adaptation for Gateway cloning in the pMDC32 expression vector, harboring a dual 35S promoter.

Arabidopsis thaliana plants were transformed according to the flower dip method (Clough and Bent, 1998). T1 transformants were selected on Murashige and Skoog medium containing 50 mg L^{–1} kanamycin and 50 mg L^{–1} hygromycin, by kanamycin only for the transformants expressing the pKGWFS7.0 vector based constructs or hygromycin only for pMDC32-based constructs. The plants were propagated under short- or long-day conditions in a cultivation room at 8 h light/20°C:16 h dark/18°C and 16 h light/20°C:8 h dark/18°C, respectively.

Yeast-two-hybrid assays

The full-length cDNAs encoding Arabidopsis *NASP.1^{SIM3.1}* and ASF1A were cloned into the pGBKT7 vector as baits and the sequences encoding full-length histones H3.1, H3.3, CenH3, H2A.W.6 and H1.3 were cloned into the pGADT7 vector as prey. Vectors pGBKT7 and pGADT7 were respectively transformed into *Saccharomyces cerevisiae* Y187 and AH109 strains based on the manufacturer's instructions of the MatchMaker III GAL4 two-hybrid system (Clontech; TaKaRa, <https://www.takarabio.com>). Screening and interaction studies between preys and baits were performed by mating compatible yeast strains following Clontech's instructions. Interactions between *NASP^{SIM3}*, ASF1A and different histones were determined by growing transformants on medium YNB without Leu and Trp (PM: permissive medium),

without Leu, Trp and His (LSM: low stringency medium) and without Leu, Trp, His and Ade (HSM: high stringency medium). Interaction efficiencies were recorded using drop tests on PM, LSM or HSM medium, with serial dilutions of a given strain grown in medium and incubated at 30°C.

To identify yet unknown interaction partners of NASP.1^{SIM3.1}, the Walker two-hybrid cDNA library CD4–10 was screened using the pGBKT7-*NASP.1^{SIM3.1}* vector as bait. Positive clones were identified by growth on high stringency medium. Among about 3×10^5 transformants, 10 positive clones were identified and sequenced. Among the potential candidates, only two proteins (NAP1;2: AT2G19480 and TSA1: AT1G52410) were subsequently analyzed, after cloning full-length CDS in the pGADT7 vector, to produce NAP1;2 and TSA1 prey constructs.

Bimolecular fluorescence complementation

The binary BiFC plant transformation vectors pSPYNE-35SGW and pSPYCE-35SGW, containing the N- or C-terminus of YFP, respectively, were kindly provided by Klaus Harter (University of Tübingen, Germany). The entire coding regions of *NASP.1^{SIM3.1}* and *CenH3* or regions coding for the N- or C-terminal parts of CenH3 (Lermontova *et al.*, 2006), respectively were subcloned from the corresponding pDONR221 vector into the BiFC vectors in frame with the split YFP. BiFC was performed in *N. benthamiana* plants (4 weeks after sowing) after *Agrobacterium*-mediated transient transformation of very young leaves containing mitotic cells according to Walter *et al.* (2004).

Proteomic analysis of Arabidopsis inflorescences expressing gCenH3–EYFP or EYFP only

Co-IP experiments were conducted on four independent inflorescent protein extracts each from gCenH3–EYFP and EYFP only expressing plants using GFP-Trap_MA Kit (Chromotek, <https://www.chromotek.com>) according manufacturer's instructions with minor modifications. Here, 150–200 inflorescences per sample were ground to a fine powder in liquid nitrogen and resuspended in ice-cold lysis or RIPA buffer (supplemented with DNase I, MgCl₂, Halt™ protease and phosphatase inhibitor cocktail; Thermo Fisher Scientific #78440). Extracts were mixed with ice-cold dilution buffer (supplemented with Halt™ Protease and phosphatase inhibitor cocktail) and pre-cleared for 45' at 4°C with equilibrated blocked magnetic-agarose beads (Chromotek). Co-IPs were performed by incubating pre-cleared extracts for 90 min to 2 h with equilibrated GFP-trap beads (Chromotek) at 4°C followed by washes to remove non-specific proteins (twice in ice-cold dilution buffer, once in ice-cold wash buffer '175 mM' (10 mM Tris/HCl pH 7.5, 0.5 mM EDTA, 175 mM NaCl) and '150 mM' (10 mM Tris/HCl pH 7.5, 0.5 mM EDTA, 150 mM NaCl) and six times in ice-cold wash buffer '100 mM' (10 mM Tris/HCl pH 7.5, 0.5 mM EDTA, 100 mM NaCl). Mass spectrometry (MS) analysis was performed as described in Data S1.

TAP and mass spectrometry experiments

Tandem affinity purifications with Arabidopsis cell cultures overexpressing CenH3 or H3.1 fused with GSRhino were performed as described earlier (Van Leene *et al.*, 2011). To prepare the construct used for expression of H3.1 and CenH3 in cell culture, genomic sequences of CENH3 and H3.1 (At1g09200) were cloned in pDONRP2R_P3 vectors via Gateway BP reaction (Invitrogen, <http://www.thermofisher.com/invitrogen>). pDONRP2R_P3 carrying CenH3 or H3.1 vectors were recombined with pDONRP4_P1R carrying 35s promoter and pDONR221 carrying GSRhino coding

sequences via Gateway LR reaction (Invitrogen) into destination vector pK7m34GW.

Nuclear protein extraction and western blot analysis

For extracts containing nuclear histones, nuclei were prepared from 2 g of 10-day-old plantlets of wild-type, *NASP.1^{SIM3.1}* RNAi line 4 and the amiRNA line 22 using HONDA buffer (20 mM Tris–HCl pH 7.4, 10 mM MgCl₂, 0.4 M sucrose, 2.5% Ficoll, 5% Dextran 40, 0.5% Triton X-100, 10 mM BSA, 0.5 mM phenylmethylsulfonyl fluoride (PMSF) and protease inhibitors (Complete Mini; Roche, <https://www.roche.com>). Nuclei were resuspended in Laemmli buffer. SDS–PAGE and western blots were performed according to standard procedures. CenH3 proteins were revealed with anti-CenH3 antibody (1/3000; Novus Biologicals, NBP1-18694, Batch 15B6, <https://www.novusbio.com>) and normalized to total H4 histones detected with an anti-H4 antibody (1/1000; Abcam, ab10158, batch GR322705-1, <https://www.abcam.com>). Primary antibodies were revealed by incubation with a horseradish peroxidase-coupled anti-rabbit secondary antibody (1/5000; Abliance, Compiègne, France, BI 2407, batch 14052, <https://www.abliance.com>). Band intensities were quantified using Multi Gauge software (Fujifilm, Tokyo, Japan, www.fujifilm.com).

Histochemical GUS enzyme activity assay

GUS activity was detected using 5-bromo-4-chloro-3-indolyl-β-D-glucuronide (Jefferson *et al.*, 1987) as described in Heckmann *et al.* (2011). A Nikon SMZ1500 stereomicroscope, equipped with a Nikon Digital Sight DS-SMc camera was used to acquire GUS images via the Nikon NIS-Elements AR 3.2x software (Nikon, <https://www.nikon.com>).

Immunostaining

4C leaf interphase nuclei were flow sorted according to Weissahrt *et al.* (2016). Immunostaining of nuclei and chromosomes was performed as described (Jasencakova *et al.*, 2000). CenH3 protein was detected with rabbit (1:2000; LifeTein, <https://www.lifetein.com>) polyclonal antisera against N-terminal peptide of CenH3 (Talbert *et al.*, 2002) and with goat anti-rabbit rhodamine (1:200; Jackson Immuno Research Laboratories, <https://www.jacksonimmuno.com>).

RNA isolation and RT-qPCR analysis

Total RNAs were extracted from shock-frozen 10-day-old wild-type seedlings as well as *NASP.1^{SIM3.1}* RNAi and amiRNA lines using RNeasy (MRC, <https://www.mrcgene.com>). Reverse transcription was primed with oligo(dT)15 using M-MLV reverse transcriptase (Promega, <https://france.promega.com>). Transcript levels were determined by quantitative polymerase chain reaction (qPCR) with the LightCycler® 480 SYBR Green I Master kit (Roche, <https://lifescience.roche.com>) on the Roche LightCycler® 480 and normalized to *MON1* (At2g28390) transcript levels, using the comparative threshold cycle method.

Microscopy

For time-lapse microscopy, seedlings were grown in coverslip chambers (Nalge Nunc International, <https://www.thermofisher.com/nalgene>) for 7–10 days and analyzed with a LSM 510 META confocal laser-scanning microscope (Carl Zeiss GmbH). EYFP was excited with a 488nm laser line and the specific fluorescence recorded with a 505–550 nm band-pass filter.

Bleaching experiments were performed with the same microscope. Nuclei were observed using a 63x/1.4 Oil Plan-Apochromat

objective (4x zoom, image size 512 × 186–232 pixels). For imaging (pre- and post-bleaching) 1.1–1.8% of a 488nm line from a 100 W argon ion laser running at 50% power was used. The emission was registered with a 505–550 band-pass filter with a maximal opened detector pinhole. Three data points were acquired to measure the pre-bleaching intensity. A small 2 × 2 µm area was photobleached using 100% of a 488nm line with five to seven iterations. The bleaching scans lasted from 50 msec (reiterated bleaching), to 250–350 msec for single and repeated FRAP experiments. Imaging scans were performed with 350 msec intervals.

To analyze the ultrastructure of immunosignals and chromatin beyond the classical Abbe/Raleigh limit at a lateral resolution of ~120 nm (super-resolution, achieved with a 488 nm laser) spatial structured illumination microscopy (3D-SIM) was applied using a 63x/1.4 Oil Plan-Apochromat objective of an Elyra PS.1 microscope system and the software ZENblack (Carl Zeiss GmbH, <https://www.zeiss.com>). Images were captured separately for each fluorochrome using the 561, 488 and 405 nm laser lines for excitation and appropriate emission filters (Weisshart *et al.*, 2016). Maximum intensity projections of whole nuclei were calculated via the ZEN software. Enlarged image sections were presented as single slices to indicate the subnuclear chromatin and protein structures at the super-resolution level. Imaris 8.0 (Bitplane, <http://www.bitplane.com>) was applied to measure the amount of CenH3 in wild-type and NASP.1^{SIM3.1} RNAi interphase nuclei via the sum of voxel intensities.

DATA AVAILABILITY STATEMENT

The authors responsible for distribution of materials integral to the findings presented in this article in accordance with the policy described in the Instructions for Authors are: Aline Probst (aline.probst@uca.fr) and Inna Lermontova (lermonto@ipk-gatersleben.de).

ACKNOWLEDGEMENTS

We thank Oda Weiss, Katrin Kumke, Jérémie Douet and Kevin Saintis for technical assistance, Jörg Fuchs for flow sorting of nuclei and Julie-Sophie Himpe for help with preparation of figures and S. Amiard for critical reading of the manuscript. We also thank VIB AP-MS platform for their help in TAP-TAG experiments. This work was supported by the Deutsche Forschungsgemeinschaft (LE2299/1–2), German Federal Ministry of Education and Research (Plant 2030, Project 031B0192NN, HaploTools), Agence National de Recherche [‘Dynam’Het’ ANR-11 JSV2 009 01, ‘SINU-DYN’ A NR-12 ISV6 0001 to AVP], Architec project (SCUSI-Région Auvergne Rhône Alpes 2017) and European Regional Development Fund-Project ‘MSCAfellow@MUNI’ (No. CZ.02.2.69/0.0/0.0/17_050/0008496). BN.K. was supported by the project from the Ghent University Special Research Fund (Grant number 01J11415), H.J. – by European Regional Development Fund Project “Plants as a tool for sustainable global development” (CZ.02.1.01/0.0/0.0/16_019/0000827). The authors would like to acknowledge networking support from COST Action CA16212 (http://www.cost.eu/COST_Actions/ca/CA16212).

CONFLICTS OF INTEREST

The authors declare no conflicts of interest.

AUTHOR CONTRIBUTIONS

AVP, DG, IL and SLG designed the research. SLG, BNK, HJ, SH, TR, SC, VS, ER, KM, AVP, IL performed experiments.

SLG, BN K, SH, SC, CHF, CT, AH, DG, IL and AVP analyzed data. AVP and IL wrote and revised the manuscript. All authors read and approved the final manuscript.

SUPPORTING INFORMATION

Additional Supporting Information may be found in the online version of this article.

Figure S1. NASP^{SIM3} protein sequence.

Figure S2. Expression profile of CenH3 and NASP^{SIM3}.

Figure S3. The NASP^{SIM3} gene codes for two different splice variants.

Figure S4. NASP^{SIM3} is a soluble protein.

Figure S5. Seed set is slightly reduced in plants with reduced NASP^{SIM3} expression.

Figure S6. Flow cytometry analysis of nuclei isolate from F1 seeds generated by crossing of NASP^{SIM3} RNAi plants with wild-type.

Video S1. NASP.1^{SIM3.1} dynamics in *Arabidopsis thaliana* root tip meristem.

Table S1. Primers used in this study.

Data S1. Supplemental methods.

REFERENCES

- Apta-Smith, M.J., Hernandez-Fernaund, J.R. and Bowman, A.J. (2018) Evidence for the nuclear import of histones H3.1 and H4 as monomers. *EMBO J.* **37**, e98714.
- Barnhart, M.C., Kuich, P.H.J.L., Stellfox, M.E., Ward, J.A., Bassett, E.A., Black, B.E. and Foltz, D.R. (2011) HJURP is a CENP-A chromatin assembly factor sufficient to form a functional de novo kinetochore. *J. Cell Biol.* **194**, 229–243.
- Batzenschlager, M., Masoud, K., Janski, N. *et al.* (2013) The GIP gamma-tubulin complex-associated proteins are involved in nuclear architecture in *Arabidopsis thaliana*. *Front. Plant Sci.* **4**, 480.
- Batzenschlager, M., Lermontova, I., Schubert, V. *et al.* (2015) Arabidopsis MZT1 homologs GIP1 and GIP2 are essential for centromere architecture. *Proc. Natl Acad. Sci. USA*, **112**, 8656–8660.
- Benoit, M., Simon, L., Desset, S., Duc, C., Cotterell, S., Poulet, A., Goff, S.Le, Tatout, C. and Probst, A.V. (2019) Replication-coupled histone H3.1 deposition determines nucleosome composition and heterochromatin dynamics during Arabidopsis seedling development. *New Phytol.* **221**, 385–398.
- Bowman, A., Lercher, L., Singh, H.R., Zinne, D., Timinszky, G., Carlomagno, T. and Ladurner, A.G. (2016) The histone chaperone sNASP binds a conserved peptide motif within the globular core of histone H3 through its TPR repeats. *Nucleic Acids Res.* **44**, 3105–3117.
- Campos, E.I., Fillingham, J., Li, G. *et al.* (2010) The program for processing newly synthesized histones H3.1 and H4. *Nat. Struct. Mol. Biol.* **17**, 1343–1351.
- Chen, Y., Baker, R.E., Keith, K.C., Harris, K., Stoler, S.A.M. and Fitzgerald-Hayes, M. (2000) The N terminus of the centromere H3-like protein Cse4p performs an essential function distinct from that of the histone fold domain. *Mol. Cell. Biol.* **20**, 7037–7048.
- Chen, C.-C., Dechassa, M.L., Bettini, E., Ledoux, M.B., Belisario, C., Heun, P., Luger, K. and Mellone, B.G. (2014) CAL1 is the Drosophila CENP-A assembly factor. *J. Cell Biol.* **204**, 313–329.
- Clough, S.J. and Bent, A.F. (1998) Floral dip: a simplified method for *Agrobacterium*-mediated transformation of *Arabidopsis thaliana*. *Plant J.* **16**, 735–743.
- Cook, A.J., Gurard-Levin, Z.A., Vassias, I. and Almouzni, G. (2011) A specific function for the histone chaperone NASP to fine-tune a reservoir of soluble H3–H4 in the histone supply chain. *Mol. Cell.* **44**, 918–927.
- De Koning, L., Corpet, A., Haber, J.E. and Almouzni, G. (2007) Histone chaperones: an escort network regulating histone traffic. *Nat. Struct. Mol. Biol.* **14**, 997–1007.
- Duc, C., Benoit, M., Goff, S.Le, Simon, L., Poulet, A., Cotterell, S., Tatout, C. and Probst, A.V. (2015) The histone chaperone complex HIR maintains nucleosome occupancy and counterbalances impaired histone deposition in CAF-1 complex mutants. *Plant J.* **81**, 707–722.

- Dunleavy, E.M., Pidoux, A.L., Monet, M., Bonilla, C., Richardson, W., Hamilton, G.L., Ekwali, K., McLaughlin, P.J. and Allshire, R.C. (2007) A NASP (N1/N2)-related protein, Sim3, binds CENP-A and is required for its deposition at fission yeast centromeres. *Mol. Cell*, **28**, 1029–1044.
- Dunleavy, E.M., Roche, D., Tagami, H., Lacoste, N., Ray-Gallet, D., Nakamura, Y., Daigo, Y., Nakatani, Y. and Almouzni-Pettinotti, G. (2009) HJURP is a cell-cycle-dependent maintenance and deposition factor of CENP-A at centromeres. *Cell*, **137**, 485–497.
- Fang, Y. and Spector, D.L. (2005) Centromere positioning and dynamics in living Arabidopsis plants. *Mol. Biol. Cell*, **16**, 5710–5718.
- Foltz, D.R., Jansen, L.E., Bailey, A.O., Iii, J.R.Y., Bassett, E.A., Wood, S., Black, B.E. and Cleveland, D.W. (2009) Centromere-specific assembly of CENP-A nucleosomes is mediated by HJURP. *Cell*, **137**, 472–484.
- Hammond, C.M., Stromme, C.B., Huang, H., Patel, D.J. and Groth, A. (2017) Histone chaperone networks shaping chromatin function. *Nat. Rev. Mol. Cell Biol.*, **18**, 141–158.
- Heckmann, S., Lermontova, I., Berckmans, B., Veylder, L.De, Bäuml, H. and Schubert, I. (2011) The E2F transcription factor family regulates CENH3 expression in *Arabidopsis thaliana*. *Plant J.*, **68**, 646–656.
- Hennig, L., Bouvet, R. and Grussem, W. (2005) MSI1-like proteins: an escort service for chromatin assembly and remodeling complexes. *Trends Cell Biol.*, **15**, 295–302.
- Janski, N., Masoud, K., Batzenschlager, M., Herzog, E., Evrard, J.-L., Houlne, G., Bourge, M., Chabouté, M.-E. and Schmit, A.-C. (2012) The GCP3-interacting proteins GIP1 and GIP2 are required for γ -tubulin complex protein localization, spindle integrity, and chromosomal stability. *Plant Cell*, **24**, 1171–1187.
- Jasencakova, Z., Scharf, A.N.D., Ask, K., Corpet, A., Imhof, A., Almouzni, G. and Groth, A. (2010) Replication stress interferes with histone recycling and predeposition marking of new histones. *Mol. Cell*, **37**, 736–743.
- Jasencakova, Z., Meister, A., Walter, J., Turner, B.M. and Schubert, I. (2000) Histone H4 acetylation of euchromatin and heterochromatin is cell cycle dependent and correlated with replication rather than with transcription. *Plant Cell*, **12**, 2087–2100.
- Jefferson, R.A., Kavanagh, T.A. and Bevan, M.W. (1987) GUS fusions: beta-glucuronidase as a sensitive and versatile gene fusion marker in higher plants. *EMBO J.*, **6**, 3901–3907.
- Jiang, D. and Berger, F. (2017) DNA replication-coupled histone modification maintains Polycomb gene silencing in plants. *Science*, **357**, 1146–1149.
- Jiang, Y., Yang, B., Harris, N.S. and Deyholos, M.K. (2007) Comparative proteomic analysis of NaCl stress-responsive proteins in Arabidopsis roots. *J. Exp. Bot.*, **58**, 3591–3607.
- Kaya, H., Shibahara, K.I., Taoka, K.I., Iwabuchi, M., Stillman, B. and Araki, T. (2001) FASCIATA genes for chromatin assembly factor-1 in Arabidopsis maintain the cellular organization of apical meristems. *Cell*, **104**, 131–142.
- Lacoste, N., Woolfe, A., Tachiwana, H., Garea, A.V., Barth, T., Cantaloube, S., Kurumizaka, H., Imhof, A. and Almouzni, G. (2014) Mislocalization of the centromeric histone variant CenH3/CENP-A in human cells depends on the chaperone DAXX. *Mol. Cell*, **53**, 631–644.
- Lermontova, I., Schubert, V., Fuchs, J., Klatte, S., Macas, J. and Schubert, I. (2006) Loading of Arabidopsis centromeric histone CENH3 occurs mainly during G2 and requires the presence of the histone fold domain. *Plant Cell*, **18**, 2443–2451.
- Lermontova, I., Fuchs, J., Schubert, V. and Schubert, I. (2007) Loading time of the centromeric histone H3 variant differs between plants and animals. *Chromosoma*, **116**, 507–510.
- Lermontova, I., Koroleva, O., Rutten, T., Fuchs, J., Schubert, V., Moraes, I., Koszegi, D. and Schubert, I. (2011) Knockdown of CENH3 in Arabidopsis reduces mitotic divisions and causes sterility by disturbed meiotic chromosome segregation. *Plant J.*, **68**, 40–50.
- Lermontova, I., Sandmann, M., Mascher, M., Schmit, A.-C. and Chabouté, M.-E. (2015) Centromeric chromatin and its dynamics in plants. *Plant J.*, **83**, 4–17.
- Liu, Z., Zhu, Y., Gao, J., Yu, F., Dong, A. and Shen, W.-H. (2009) Molecular and reverse genetic characterization of NUCLEOSOME ASSEMBLY PROTEIN1 (NAP1) genes unravels their function in transcription and nucleotide excision repair in *Arabidopsis thaliana*. *Plant J.*, **59**, 27–38.
- Maksimov, V., Nakamura, M., Wildhaber, T., Nanni, P., Ramström, M., Bergquist, J. and Hennig, L. (2016) The H3 chaperone function of NASP is conserved in Arabidopsis. *Plant J.*, **88**, 425–436.
- Mattioli, F., D'Arcy, S. and Luger, K. (2015) The right place at the right time: chaperoning core histone variants. *EMBO Rep.*, **16**, 1454–1466.
- Müller, S. and Almouzni, G. (2017) Chromatin dynamics during the cell cycle at centromeres. *Nat. Rev. Genet.*, **18**, 192–208.
- Nabeel-Shah, S., Ashraf, K., Pearlman, R.E. and Fillingham, J. (2014) Molecular evolution of NASP and conserved histone H3/H4 transport pathway. *BMC Evol. Biol.*, **14**, 139.
- Nakaminami, K., Matsui, A., Nakagami, H. et al. (2014) Analysis of differential expression patterns of mRNA and protein during cold-acclimation and de-acclimation in Arabidopsis. *Mol. Cell Proteomics*, **13**, 3602–3611.
- Natsume, R., Eitoku, M., Akai, Y. and Sano, N. (2007) Structure and function of the histone chaperone CIA/ASF1 complexed with histones H3 and H4. *Nature*, **446**, 1–4.
- Okada, M., Cheeseman, I.M., Hori, T., Okawa, K., McLeod, I.X., Yates, J.R., Desai, A. and Fukagawa, T. (2006) The CENP-H-I complex is required for the efficient incorporation of newly synthesized CENP-A into centromeres. *Nat. Cell Biol.*, **8**, 446–457.
- Osakabe, A., Tachiwana, H., Matsunaga, T., Shiga, T., Nozawa, R.S., Obuse, C. and Kurumizaka, H. (2010) Nucleosome formation activity of human somatic nuclear autoantigenic sperm protein (sNASP). *J. Biol. Chem.*, **285**, 11913–11921.
- Phansalkar, R., Lapierre, P. and Mellone, B.G. (2012) Evolutionary insights into the role of the essential centromere protein CAL1 in Drosophila. *Chromosome Res.*, **20**, 493–504.
- Pidoux, A.L., Choi, E.S., Abbott, J.K.R. et al. (2009) Article fission yeast Scm3: a CENP-A receptor required for integrity of subkinetochore chromatin. *Mol. Cell*, **33**, 299–311.
- Ravi, M. and Chan, S.W.L. (2010) Haploid plants produced by centromere-mediated genome elimination. *Nature*, **464**, 615–618.
- Ravi, M., Shibata, F., Ramahi, J.S., Nagaki, K., Chen, C., Murata, M. and Chan, S.W.L. (2011) Meiosis-specific loading of the centromere-specific histone CENH3 in *Arabidopsis thaliana*. *PLoS Genet.*, **7**, e1002121.
- Ren, J., Wen, L., Gao, X., Jin, C., Xue, Y. and Yao, X. (2009) DOG 1.0: illustrator of protein domain structures. *Cell Res.*, **19**, 271.
- Richardson, R.T., Batova, I.N., Widgren, E.E., Zheng, L., Whitfield, M., Marzluff, W.F. and Rand, M.G.O. (2000) Characterization of the histone H1-binding protein, NASP, as a cell cycle-regulated somatic protein. *J. Biol. Chem.*, **275**, 30378–30386.
- Rosin, L.F. and Mellone, B.G. (2017) Centromeres drive a hard bargain. *Trends Genet.*, **33**, 101–117.
- Schwab, R., Ossowski, S., Riester, M., Warthmann, N. and Weigel, D. (2006) Highly specific gene silencing by artificial microRNAs in Arabidopsis. *Plant Cell*, **18**, 1121–1133.
- Stoler, S., Rogers, K., Weitz, S., Morey, L., Fitzgerald-Hayes, M. and Baker, R.E. (2007) Scm3, an essential *Saccharomyces cerevisiae* centromere protein required for G2/M progression and Cse4 localization. *Proc. Natl Acad. Sci. USA*, **104**, 10571–10576.
- Suzuki, T., Nakajima, S., Morikami, A. and Nakamura, K. (2005) An Arabidopsis protein with a novel calcium-binding repeat sequence interacts with TONSOKU/MGOUN3/BRUSHY1 involved in meristem maintenance. *Plant Cell Physiol.*, **46**, 1452–1461.
- Talbert, P.B., Masuelli, R. and Tyagi, A. (2002) Centromeric localization and adaptive evolution of an Arabidopsis histone H3 variant. *Plant Cell*, **14**, 1053–1066.
- Talbert, P.B., Ahmad, K., Almouzni, G. et al. (2012) A unified phylogeny-based nomenclature for histone variants. *Epigenetics Chromatin*, **5**, 7.
- Tan, H.L., Lim, K.K., Yang, Q. et al. (2018) Prolyl isomerization of the CENP-A N-terminus regulates centromeric integrity in fission yeast. *Nucleic Acids Res.*, **46**, 1167–1179.
- Tripathi, A.K., Singh, K., Pareek, A. and Singla-Pareek, S.L. (2015) Histone chaperones in Arabidopsis and rice: genome-wide identification, phylogeny, architecture and transcriptional regulation. *BMC Plant Biol.*, **15**, 1–25.
- Van Leene, J., Eeckhout, D., Persiau, G., Van De Slijke, E., Geerinck, J., Van Isterdael, G., Witters, E. and De Jaeger, G. (2011) Isolation of Transcription Factor Complexes from Arabidopsis Cell Suspension Cultures by Tandem Affinity Purification BT – Plant Transcription Factors: Methods and Protocols (Yuan, L. and Perry, S.E., eds). Totowa, NJ: Humana Press, pp. 195–218.

- Walter, M., Chaban, C., Schütze, K. *et al.* (2004) Visualization of protein interactions in living plant cells using bimolecular fluorescence complementation. *Plant J.* **40**, 428–438.
- Wang, H., Ge, Z., Walsh, S.T.R. and Parthun, M.R. (2012) The human histone chaperone sNASP interacts with linker and core histones through distinct mechanisms. *Nucleic Acids Res.* **40**, 660–669.
- Weisshart, K., Fuchs, J. and Schubert, V. (2016) Structured illumination microscopy (SIM) and photoactivated localization microscopy (PALM) to analyze the abundance and distribution of RNA polymerase II molecules on flow-sorted Arabidopsis nuclei. *Bio-Protocol*, **6**, e1725.
- Zasadińska, E., Huang, J., Bailey, A.O. *et al.* (2018) Inheritance of CENP-A nucleosomes during DNA replication requires HJURP. *Dev. Cell*, **47**, 348–362.e7.
- Zhu, Y., Weng, M., Yang, Y., Zhang, C., Li, Z., Shen, W.H. and Dong, A. (2011) Arabidopsis homologues of the histone chaperone ASF1 are crucial for chromatin replication and cell proliferation in plant development. *Plant J.* **66**, 443–455.